

20 Gwd SiC Clad Fuel Pin Examination

APRIL 2014

Prepared by

R.N. Morris
C.A. Baldwin
R.J. Ellis
J.M. Giaquinto
L.J. Ott (retired)
J.L. Peterson
J.E. Schmidlin

DOCUMENT AVAILABILITY

Reports produced after January 1, 1996, are generally available free via US Department of Energy (DOE) SciTech Connect.

Website <http://www.osti.gov/scitech/>

Reports produced before January 1, 1996, may be purchased by members of the public from the following source:

National Technical Information Service
5285 Port Royal Road
Springfield, VA 22161
Telephone 703-605-6000 (1-800-553-6847)
TDD 703-487-4639
Fax 703-605-6900
E-mail info@ntis.gov
Website <http://www.ntis.gov/support/ordernowabout.htm>

Reports are available to DOE employees, DOE contractors, Energy Technology Data Exchange representatives, and International Nuclear Information System representatives from the following source:

Office of Scientific and Technical Information
PO Box 62
Oak Ridge, TN 37831
Telephone 865-576-8401
Fax 865-576-5728
E-mail reports@osti.gov
Website <http://www.osti.gov/contact.html>

This report was prepared as an account of work sponsored by an agency of the United States Government. Neither the United States Government nor any agency thereof, nor any of their employees, makes any warranty, express or implied, or assumes any legal liability or responsibility for the accuracy, completeness, or usefulness of any information, apparatus, product, or process disclosed, or represents that its use would not infringe privately owned rights. Reference herein to any specific commercial product, process, or service by trade name, trademark, manufacturer, or otherwise, does not necessarily constitute or imply its endorsement, recommendation, or favoring by the United States Government or any agency thereof. The views and opinions of authors expressed herein do not necessarily state or reflect those of the United States Government or any agency thereof.

LWRS SiC Clad Technology Development Program

20 Gwd SiC Clad Fuel Pin Examination

R.N. Morris
C.A. Baldwin
R.J. Ellis
J.M. Giaquinto
L.J. Ott (retired)
J.L. Peterson
J.E. Schmidlin

Date Published: *April 2014*

Prepared by
OAK RIDGE NATIONAL LABORATORY
Oak Ridge, Tennessee 37831-6283
managed by
UT-BATTELLE, LLC
for the
US DEPARTMENT OF ENERGY
under contract DE-AC05-00OR22725

CONTENTS

	Page
CONTENTS.....	iii
LIST OF FIGURES	iv
LIST OF TABLES.....	v
ACRONYMS.....	vi
ABSTRACT.....	1
1. FUEL PIN CONSTRUCTION AND IRRADIATION.....	1
2. Progress of the PIE Task.....	6
2.1 Capsule Trimming	6
2.2 Capsule Diameter and Surface Flaws	6
2.3 Capsule Temperature and Gamma Scan	6
2.4 Capsule Puncture	6
2.5 Open Capsule and Remove Fuel Pin.....	10
2.6 Measure Fuel Pin Temperature and Photograph.....	11
2.7 Measure Fuel Pin Diameter.....	11
2.8 Segment the Fuel Pin for MET/SEM and Radiochemical Samples.....	15
2.8.1 Measured Percent Fission (Burn-up)	22
2.8.2 Summary of Simulation Calculations and Burn-up Determinations.....	24
3. PIE CONCLUSIONS.....	27
4. ACKNOWLEDGEMENTS	27
5. REFERENCES	27

LIST OF FIGURES

Figure	Page
Figure 1. Capsule and fuel pin design. Each Capsule assembly contains one fuel pin with 10 fuel pellets (11 pellets are shown in this diagram, but 10 were used in the actual irradiation).....	3
Figure 2. Fuel pin B4 fission power history.....	4
Figure 3. Planned flow chart for PIE.	5
Figure 4. Low energy gamma scan of capsule showing the fuel stack.	7
Figure 5. High energy gamma scan showing the internal components.....	8
Figure 6. Comparison of Kr isotope concentrations in the capsule gas sample.....	10
Figure 7. Comparison of Xe isotope concentrations in the capsule gas sample.	11
Figure 8. The results of the fuel pin removal. Note that the fuel pin end plugs were stuck to the capsule inner walls and had to be pried loose.....	12
Figure 9. Photographs of the broken fuel pin. Note that the failures took place near the end plugs.	13
Figure 10. Photographs of capsule inner and outer surfaces near the top of the fuel pin. There are no indications of any large surface build-ups; only a mild discoloration.	14
Figure 11. Outer capsule and fuel pin diameters. Note the increases near the fuel pin ends. This graph does not include the fuel pin broken off end plugs.	16
Figure 12. Capsule inner and fuel pin outer diameters illustrating gap.	17
Figure 13. Clad ring sample about 1” from bottom. Difficulties were encountered in the preparation of this mount; however, some detail about the structure of the clad can be gleaned. Because of the poor nature of this mount, no information about the cracking is certain since the cracks may have occurred during the preparation; however, the clad was in poor condition prior to mounting so it is likely that some physical damage occurred during irradiation.....	18
Figure 14. Cross section of top end plug and adjacent cladding. Note the poor condition of the cladding and the uneven distribution of the fibers at the 5 o’clock position. The end plug either shifted or chipped and could not be polished flat. The cement holding the plug in is not readily apparent. The black regions are epoxy; it is difficult to tell if the SiC composite has significant porosity or if these regions are due to pull-out during preparation.	19
Figure 15. Close up of cladding region at 5 o’clock (Figure 14) with low fiber count.	20
Figure 16. Cladding region at 4 o’clock (Figure 14) showing the relative thicknesses of the three cladding regions: inner SiC seal layer, composite layer, and outer SiC seal layer.....	21
Figure 17. From Ref. 9, the rim effect in the radial fuel burn-up profile of an irradiated fuel pellet, for average pellet burn-ups from 20 to 80 GWd/MTHM. The effect is not insignificant, even for burn-up of 20 GWd/MTHM	26
Figure 18. Plutonium and Neodymium Concentrations across the radius of a fuel pellet in the Ref. 10 measurements: Illustration of the rim effect in irradiated pellets.	26

LIST OF TABLES

Table	Page
Table 1. Calculated Versus Measured Kr isotopes.	9
Table 2. Calculated Versus Measured Xe Isotopes.....	9
Table 3. Capsule and Fuel Pin Results. Note the fuel pin leaked and these measurements are not accurate representations of fuel performance.....	9
Table 4. Results: Assay (g / g Fuel) and Isotopics (wt. %) by IDMS	23
Table 5. Results: Radionuclide Bq count rates and their equivalent mass fractions (g/g Fuel).....	23
Table 6. Measured Percent Fission (Burn-up)	24
Table 7. Comparison of Selected Calculated and Measured (IDMS) Nuclide Mass Fractions	24
Table 8. Comparison of Calculated and Measured Radionuclide Mass Fractions.....	25

ACRONYMS

ADEPT	Advanced Diagnostics and Evaluation Platform Apparatus
CSU	Combined Standard Uncertainties
GWd/MTHM	Giga Watt Days per Metric Ton (initial) Heavy Metal
IDMS	Isotope Dilution Mass Spectrometry
MC-ICPMS	High precision multi-collector ICPMS
NBL	New Brunswick Laboratory
NIDC	National Isotope Development Center
PIE	Post Irradiation Examination
PWR	Pressurized Water Reactor

ABSTRACT

A test fuel pin, B4, composed of UO₂ pellets in a SiC tube cladding with SiC end plugs cemented in place with a glassy ceramic was irradiated in a stainless steel containment capsule to a burn-up of approximately 20 GWd/MTHM in the High Flux Isotope Reactor (HFIR). B4 was one of a set of fuel pins irradiated in a Hf-shielded facility inserted in a VXF site in the Be reflector. The neutron flux environment during the irradiation was designed to be consistent with that in a pressurized power reactor (PWR). After removal, post-irradiation examination (PIE) work was performed and the SiC cladding and end plugs were found to be damaged; the fuel pin was found to be fractured into three pieces. Measurements indicated greater than expected SiC swelling; the UO₂ fuel performed as expected.

1. FUEL PIN CONSTRUCTION AND IRRADIATION

A UO₂ fuel pin, designated B4, designed to test an early SiC cladding material and end plug design was constructed and encapsulated in a stainless steel capsule for irradiation in HFIR. The stainless steel capsule was a necessary safety containment feature for irradiation in HFIR. Figure 1 is a schematic of the fuel pin and its containment. [1, 2]

B4 was one of originally nine UO₂ fuel pins in the Hf-shielded B basket facility inserted into the VXF-12 site in the reflector. There is another basket facility, A, inserted into VXF-4 that contains UCN fuel pins also with SiC cladding; there were originally seven of these fuel pins undergoing irradiation in HFIR as well as two dummy (aluminum) fuel pins in Basket A. The active UO₂ and UCN fuel pins all have 10 fuel pellets. The Hf shield was designed such that the linear heat generation in the fuel pins was within a range consistent with Westinghouse PWR cores with 17×17 fuel assemblies. In the HFIR irradiations of B4 and the other fuel pins, the pins were heated by their fission power and also by gamma irradiation from the HFIR core (prompt from the fissions, and delayed γ irradiation from the build-up of fission products in the core). [3-6]

The fuel pin B4 is composed of 10 UO₂ pellets, 4.95% enrichment, in a SiC tube with SiC end plugs cemented in place with a glassy ceramic. The fuel cladding is a triplex SiC material made up of an inner monolith of chemically vapor deposited (CVD) beta phase SiC, a middle layer of stoichiometric SiC fiber impregnated with beta phase SiC, and an outer layer of CVD beta SiC. The inside diameter of the cladding is 0.329 in., and the outside diameter is 0.393 in.

This pin was then contained in a stainless steel capsule with appropriate gaps to control the pin cladding operating temperature. The temperatures and material changes are not monitored during the irradiation except for gross capsule outer diameter limits that are measured by go/no-go gauges during reactor outages.

The fuel pin capsule was irradiated for 403 full powers days in HFIR to a calculated burn-up of about 20 giga watt days per metric ton (initial) heavy metal (GWd/MTHM); it was exposed to a thermal neutron fluence of 1.378×10^{21} n/cm² and an average fuel pin clad operating temperature of about 380°C. The average fuel pin B4 burn-up per HFIR cycle is about 1.35 GWd/MTHM for the 16 cycles (HFIR cycle numbers 431 to 446) which totaled 403.19 fpd (34,271 MWd for HFIR core fission energy). The B4 fuel pin fission power history is approximately as shown in Figure 2.

After irradiation and a short cooling period, the fuel pin was transported to the Building 3525 hot cell bank for PIE work.

Eight tasks had been selected for the examination of the SiC UO₂ capsule:

1. Trim the coolant passage centering fins off the capsule without breaking the seal so it can be more easily handled;

2. Measure the capsule diameter in a few axial positions to determine if there is any significant swelling. Examine for surface flaws;
3. Measure capsule temperature. Place the capsule in a holder rod and gamma scan it in the Advanced Diagnostics and Evaluation Platform (ADEPT) apparatus;
4. Puncture the capsule, measure the pressure, free volume, and capture any ^{85}Kr and gamma count it;
5. Cut the ends off the capsule and remove the SiC clad fuel pin;
6. Measure temperature. Visually inspect the fuel pin and take macro photographs;
7. Measure the clad diameter on the fuel pin in several locations to determine its diameter as a function of length;
8. Segment the fuel pin for Metallographic (MET) / Scanning Electron Microscope (SEM) and radiochemical samples.

A flow diagram of the planned PIE is shown in Figure 3. Preparation for the PIE included the design and construction of jigs and fixtures for cutting and capsule puncturing. This equipment was developed and installed without any problems.

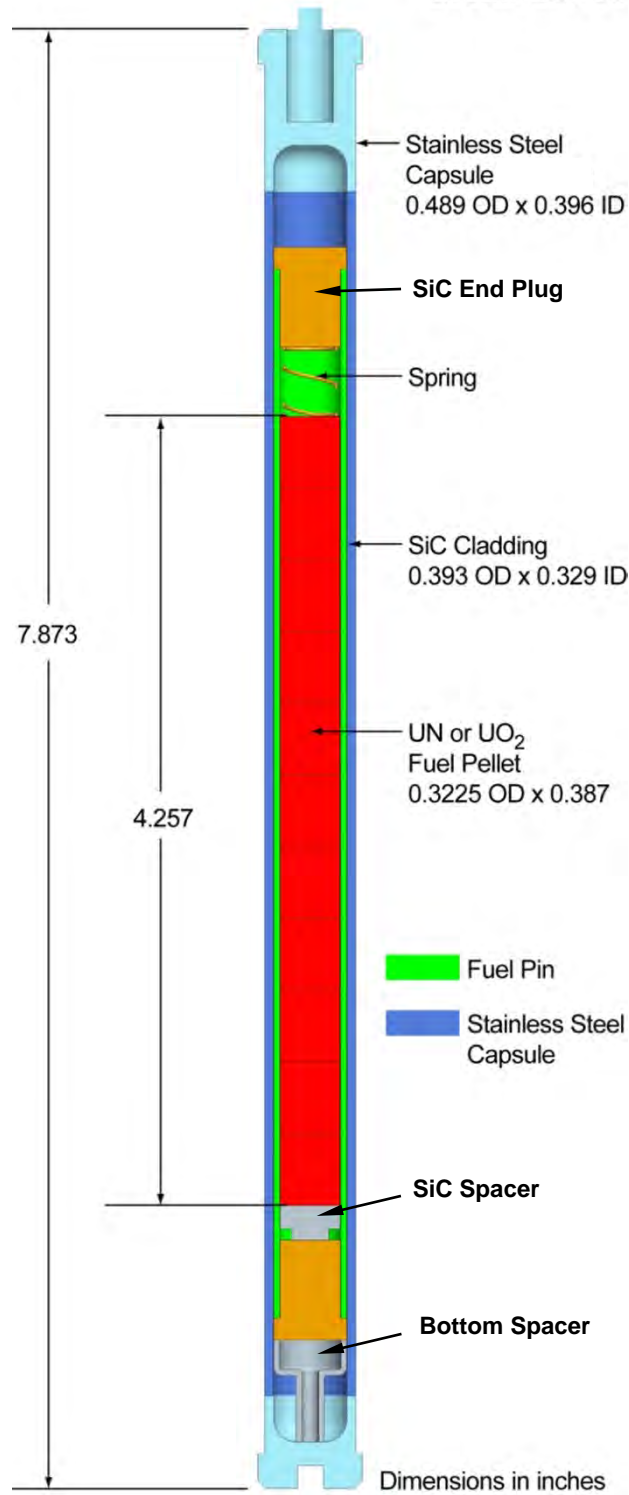


Figure 1. Capsule and fuel pin design. Each Capsule assembly contains one fuel pin with 10 fuel pellets (11 pellets are shown in this diagram, but 10 were used in the actual irradiation)

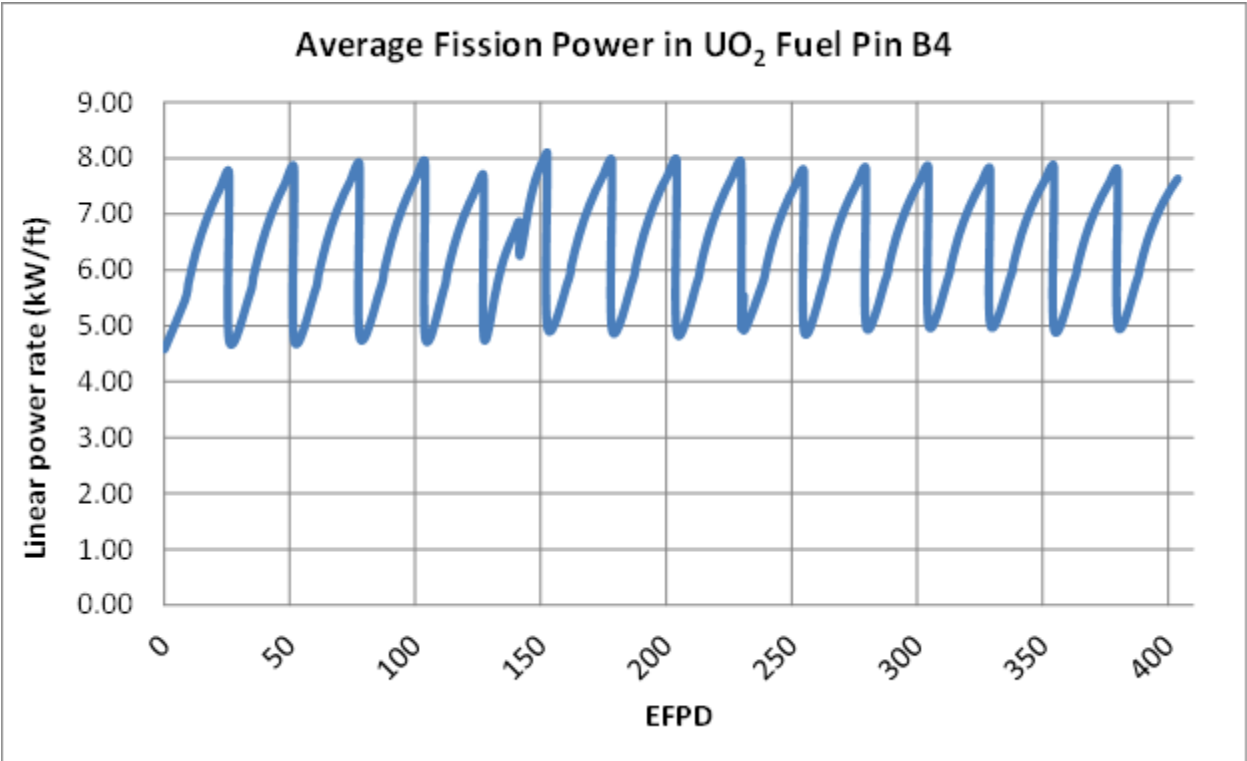


Figure 2. Fuel pin B4 fission power history.

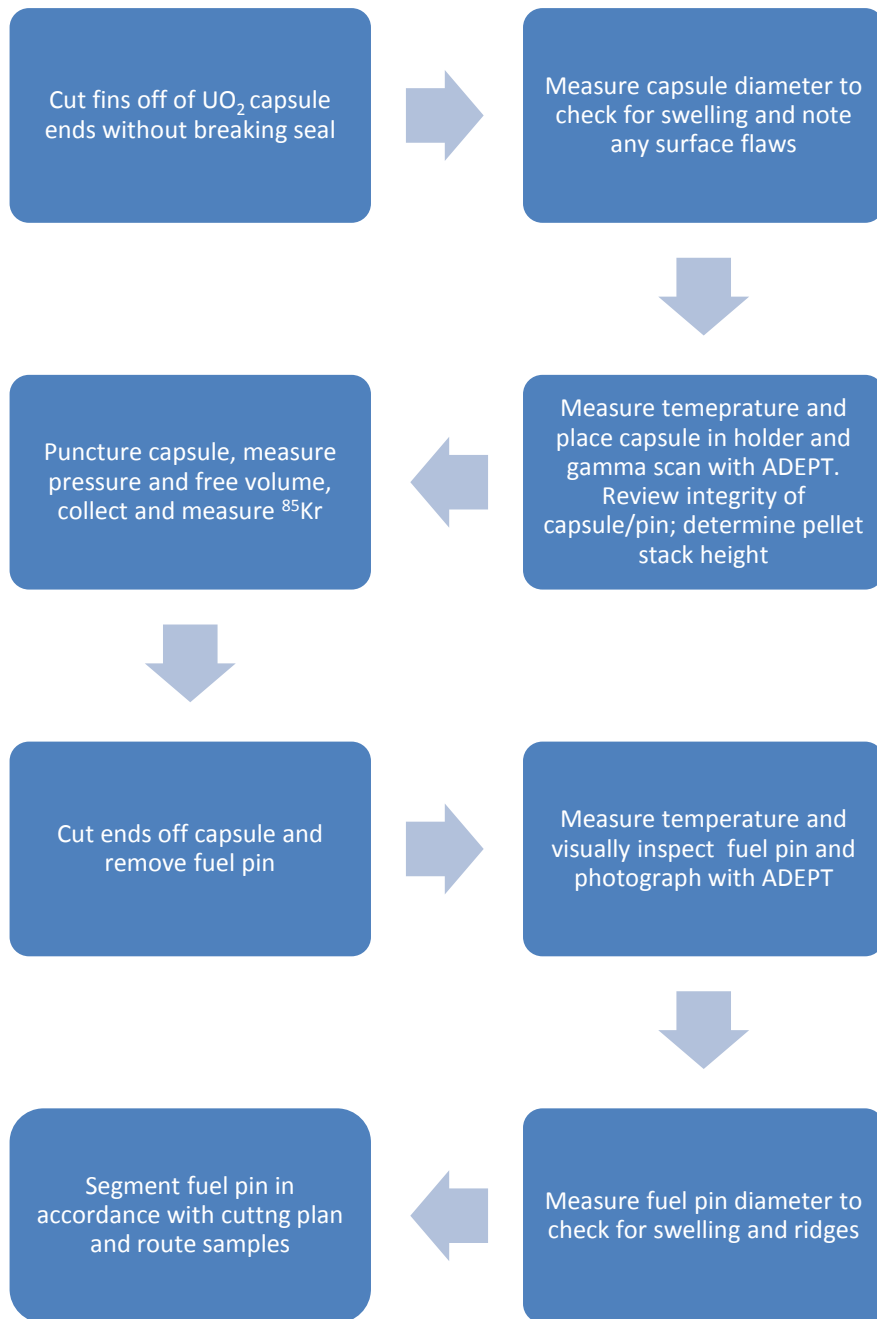


Figure 3. Planned flow chart for PIE.

2. PROGRESS OF THE PIE TASK

This section presents the PIE results as outlined in the Figure 3 flowchart.

2.1 Capsule Trimming

The end fins were trimmed off the capsule using a thin abrasive blade. The bottom set was removed just at the end of the fins to insure that the capsule seal was not broken and the top set was removed ¼” from the capsule top. A discolored surface film on the capsule was noticed at this time.

2.2 Capsule Diameter and Surface Flaws

Using a measurement jig based on SONY magnetic probes, developed for this PIE, the outer diameter of the capsule was measured. The capsule diameter was found to be larger than expected and the largest diameter was at the top of the capsule. At first this was thought to be related to the observed surface film, but later observations revealed this not to be the case. Results of the measurements will be presented in later sections.

2.3 Capsule Temperature and Gamma Scan

The capsule temperature was measured by holding it horizontal in free air with a thermocouple clamped to the approximate center of the trimmed capsule. The measured temperature of the capsule was 38.3°C; the cell ambient temperature was 35.4°C. The only non-convection air movement was due to the low flow hot cell ventilation system.

The capsule was then placed in a holder tube for alignment in the gamma scanner and gamma scanned. The data points were taken 0.04” apart with a counting time of 60s; three energy ranges were recorded: 400 to 1600KeV, 400 to 800KeV, and 1100 to 1600KeV. The scan indicated no abnormalities with the internal components. The measured fuel stack was 4.02” and the as-build fuel stack was 3.93”; they agree within the accuracy of the gamma scan. Other than a couple of small cracks/gaps, the fuel stack was in excellent condition. The 400 to 800KeV scan is shown in Figure 4 and the 1100 to 1600KeV scan is shown in Figure 5. No information about minor swelling (< 0.04”) could be obtained from the scan.

2.4 Capsule Puncture

The capsule was punctured in a device especially designed for this task. Kr-85 was seen in the capsule fill gas indicating that at some time during the irradiation the fuel pin leaked. A fraction of the capsule gas was sampled and analyzed for gas isotopes (referenced to 10 Oct 2010). See Table 1 and Table 2; agreement is reasonable for the higher mole fractions. A graphic comparison of the Kr isotopes is shown in Figure 6 and the Xe isotopes in Figure 7. The accuracy of the Kr comparison is not quite as good because of the low concentration of the Kr isotopes in the gas sample; however, the overall analysis shows good agreement between the measured and predicted mole fractions indicating that the irradiation burn-up predictions were on track.

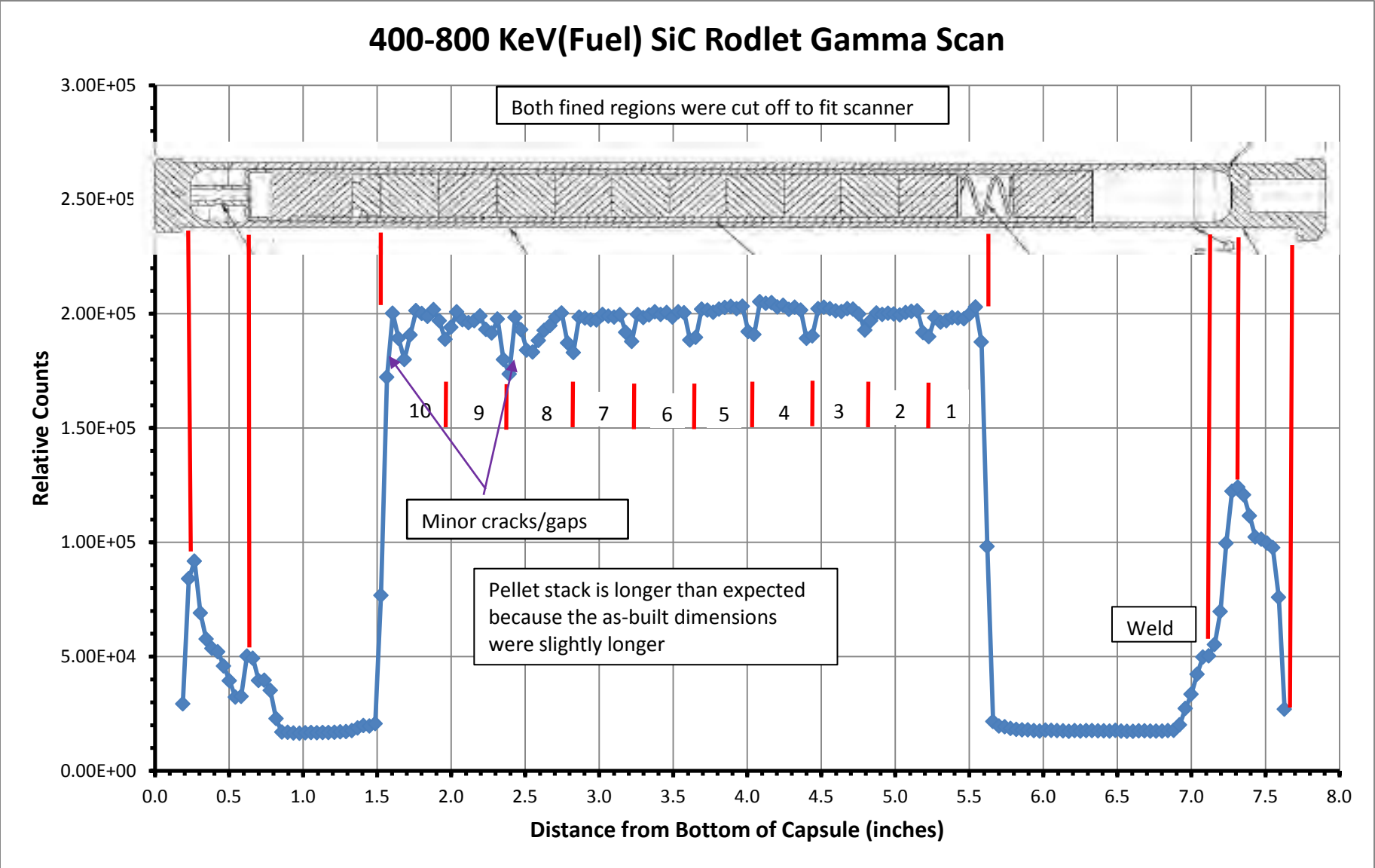


Figure 4. Low energy gamma scan of capsule showing the fuel stack.

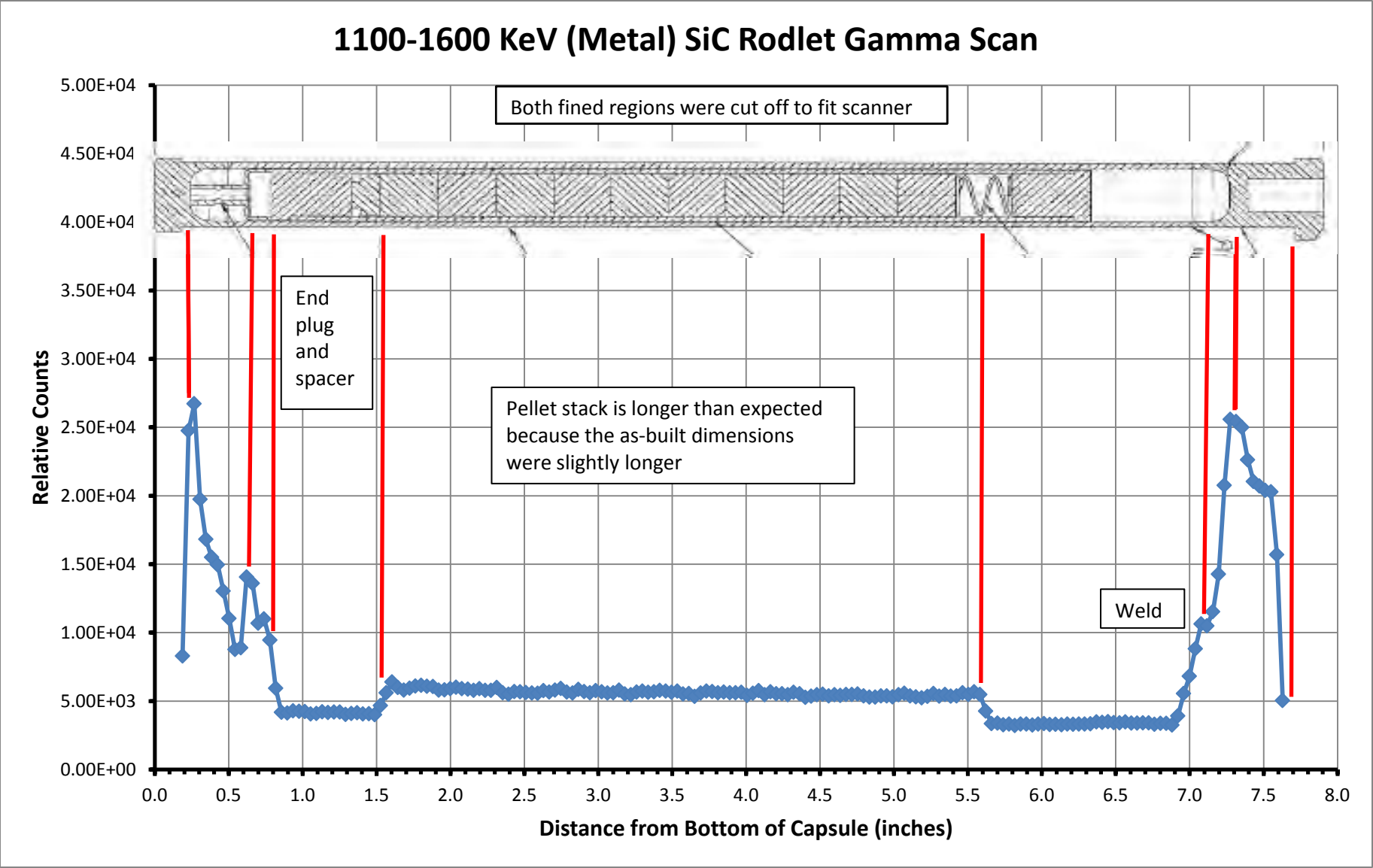


Figure 5. High energy gamma scan showing the internal components.

The measured capsule volume was 0.2 cu inches, the pressure was 28 psia, the Kr-85 inventory was 1.2×10^{-3} Ci, and the estimated fuel gas release fraction based on this measurement was 0.22%. The fuel pin clearly leaked an unknown amount at some time during irradiation; thus, these activity and pressure values are not representative of expectations since they involve unknown combinations of fuel release, pin volume, capsule fill gas, and capsule volume. See Table 3. Note however, that a fission gas isotope's *mole fraction* (previous paragraph) is little effected by this leakage issue because early in the irradiation the gas generation comes mostly from the fission of U-235; little comes from other (bred) isotopes which can have a different Kr/Xe ratio.

During assembly, there were problems with the end seals on a number of capsules and it was not possible to predict the irradiation performance of the seals in general. Thus, it is not known whether the pin leakage was due to fabrication difficulties, irradiation seal damage, or general SiC swelling [1].

Table 1. Calculated Versus Measured Kr isotopes.

Isotope	Calculated Mole Fraction	Measured Mole Fraction (< 0.1 ± 20%, > 0.1± 10%)
Kr-82	4.38E-05	4.84E-02
Kr-83	1.46E-01	1.34E-01
Kr-84	2.79E-01	4.02E-01
Kr-85	1.02E-01	4.63E-02
Kr-86	4.72E-01	3.69E-01

Table 2. Calculated Versus Measured Xe Isotopes.

Isotope	Calculated Mole Fraction	Measured Mole Fraction (< 0.1 ± 20%, > 0.1± 10%)
Xe-128	1.00E-05	2.80E-03
Xe-130	5.31E-05	8.30E-03
Xe-131	1.04E-01	1.18E-01
Xe-132	1.74E-01	2.01E-01
Xe-133	N/A	4.70E-03
Xe-134	2.92E-01	2.76E-01
Xe-136	4.29E-01	3.89E-01

Table 3. Capsule and Fuel Pin Results. Note the fuel pin leaked and these measurements are not accurate representations of fuel performance.

Item	Value
Calculated fuel pin free volume (nominal, swelling not included)	0.054 in ³
Calculated capsule free volume (nominal, distortion not included)	0.18 in ³
Sum of free volumes	0.23 in ³
Measured capsule/pin volume (from capsule puncture) ±22%	0.20 in ³
Measured pressure (from capsule puncture) ±20%	28 psia
Measured Kr-85 inventory (from capsule puncture) ±7%	1.2×10^{-3} Ci

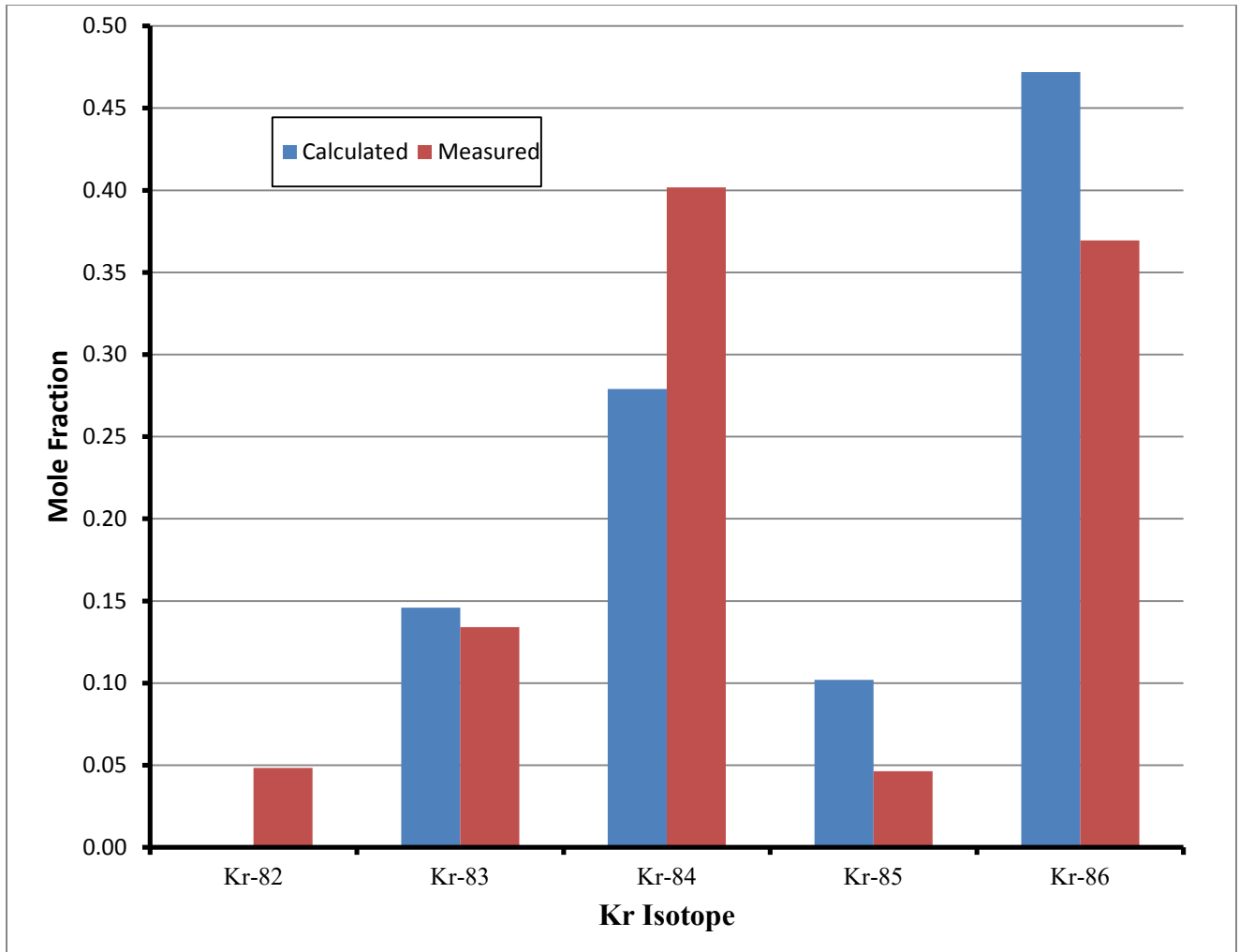


Figure 6. Comparison of Kr isotope concentrations in the capsule gas sample.

2.5 Open Capsule and Remove Fuel Pin

The capsule was opened by sawing off the ends to expose the fuel pin. The capsule was then placed in a push-out jig to remove the fuel pin; however, the pin could not be pushed out despite using a considerable amount of force. The capsule was finally opened by milling two longitudinal slots 180° apart along its length. The retrieved fuel pin was broken into 3 pieces along with a modest amount of debris. It is not clear when the pin broke; it could have broken during irradiation, handling, or during the milling to free it. The puncture results in the previous sections showed that there was a loss of pin seal at some point in the irradiation and handling. See Figure 8. The end plugs were stuck to the capsule inner walls and had to be pried loose. There was a considerable amount of debris; both broken SiC clad and fuel pellets pieces.

The fuel was loose in the clad and slid out during handling; thus, the radiochemical sample location was lost and a MET mount with both fuel and cladding could not be prepared.

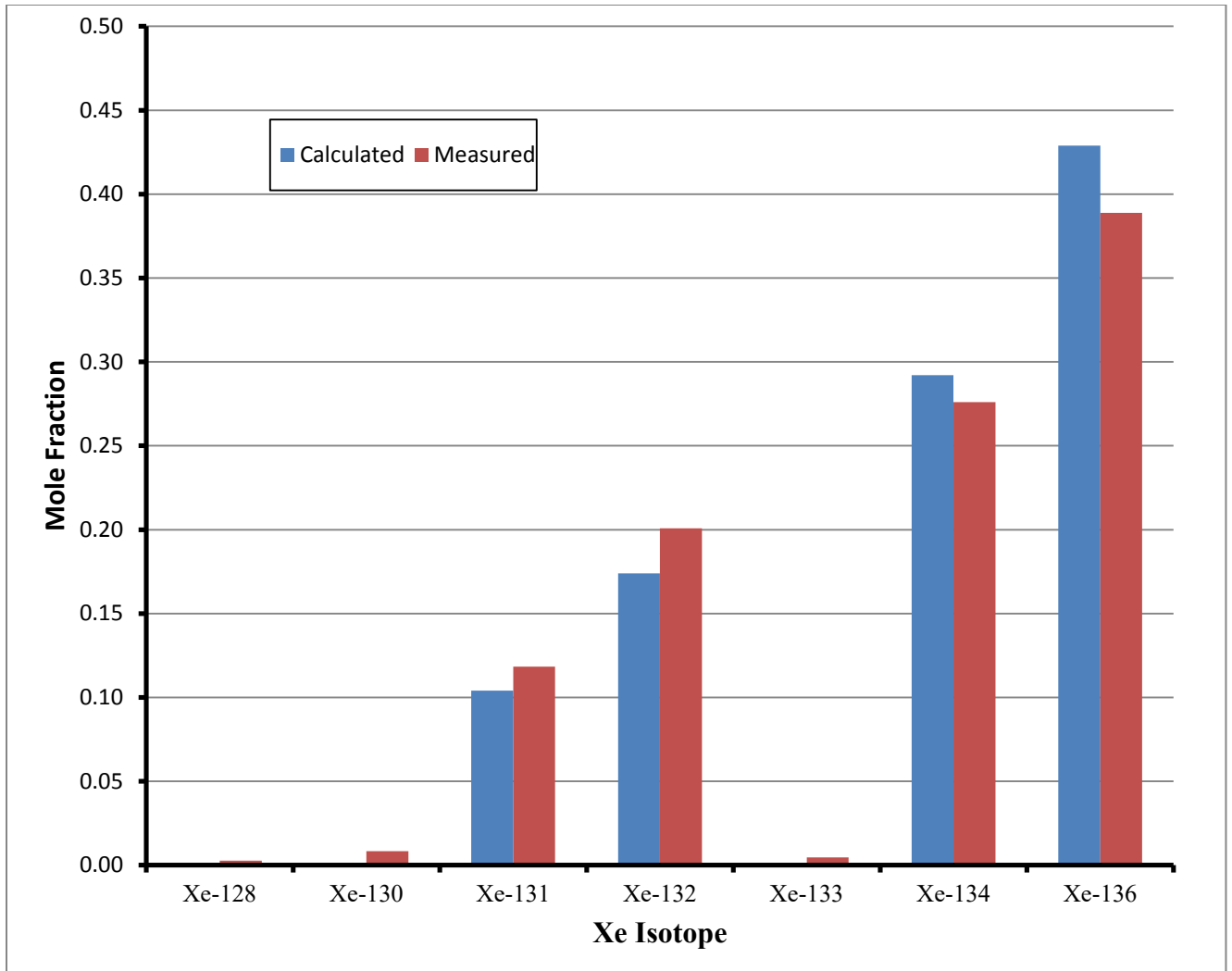


Figure 7. Comparison of Xe isotope concentrations in the capsule gas sample.

2.6 Measure Fuel Pin Temperature and Photograph

Because of the poor condition of the fuel pin the temperature was not measured for fear of spreading fuel contamination and causing further damage. Pictures were taken of the fuel pin and a portion of the capsule near the top of the fuel pin. Figure 9 shows photographs of the fuel pin. Note that the failure took place near the end plugs.

A stainless steel capsule piece near the top of the capsule was also photographed. There were no indications of any large surface build-up that might cause the capsule diameter to increase. See Figure 10.

2.7 Measure Fuel Pin Diameter

The fuel pin diameter was measured as possible using a SONY magnetic probe and a flat base plate, calibration checked with standard gauge pins. The poor condition of the pin and the release of fuel debris probably increased the error of the measurements, but a reasonably consistent set of values was obtained.

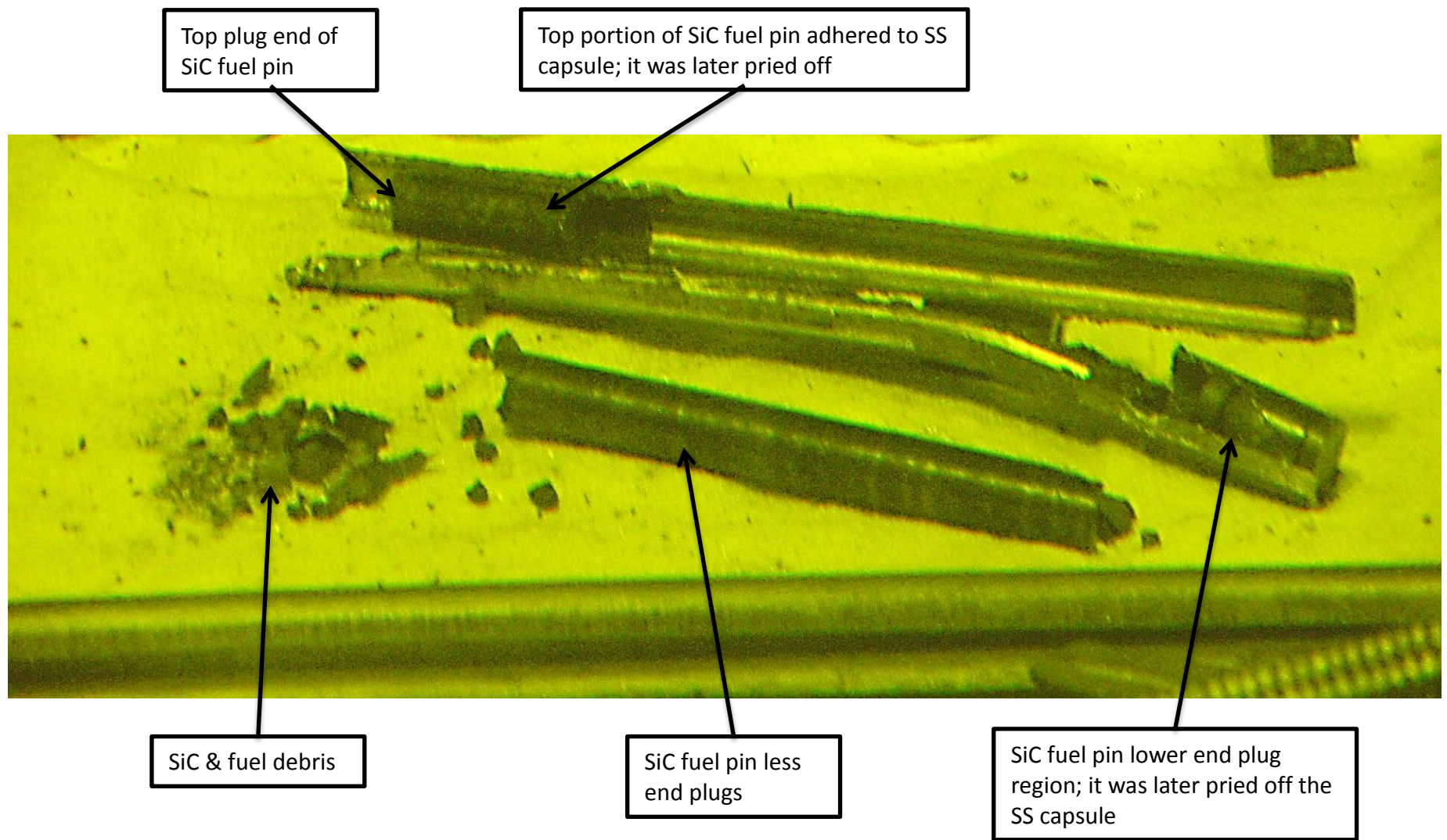
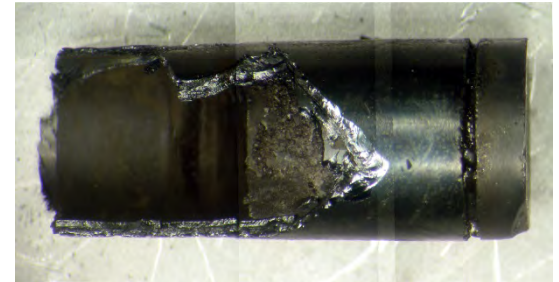
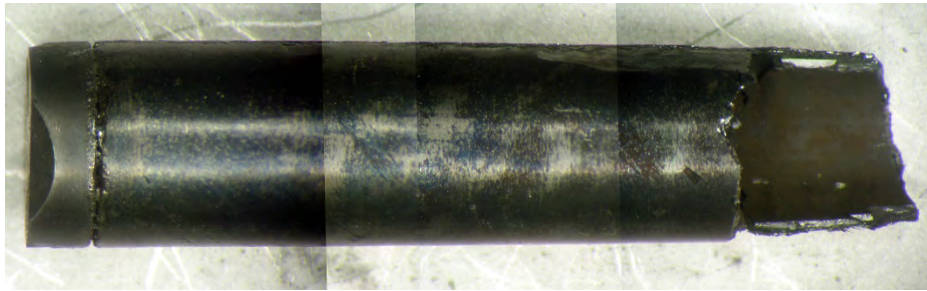
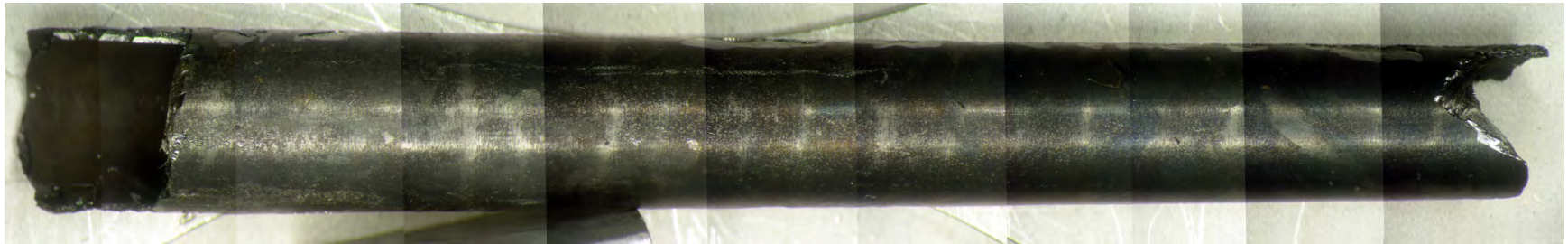


Figure 8. The results of the fuel pin removal. Note that the fuel pin end plugs were stuck to the capsule inner walls and had to be pried loose.

Fueled Region



Top Plenum

Bottom End Plug

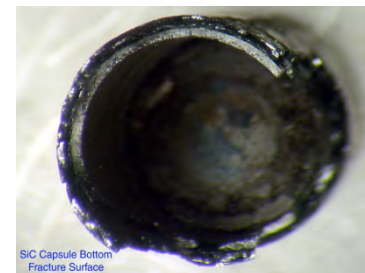
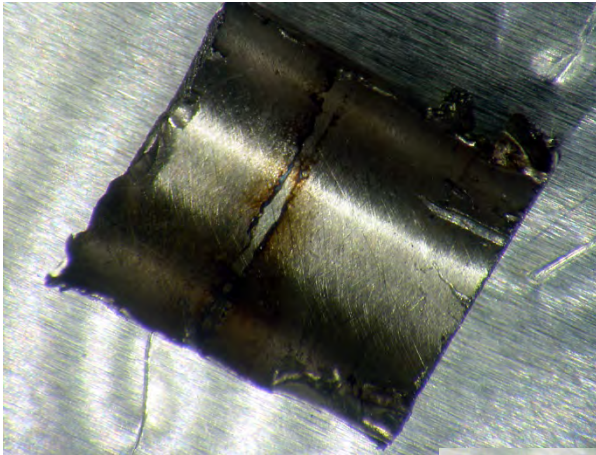
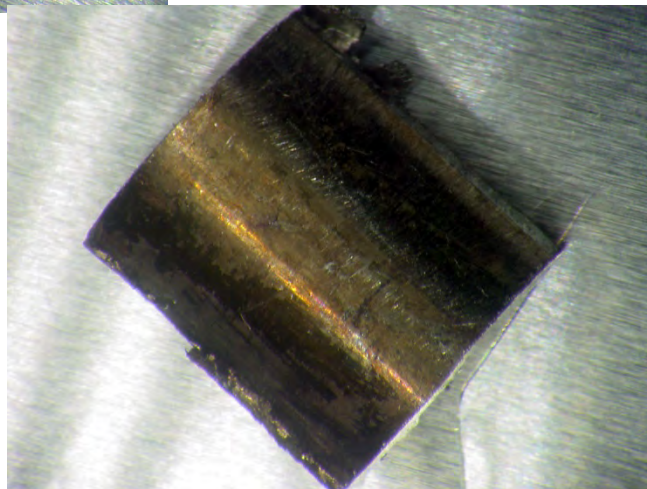


Figure 9. Photographs of the broken fuel pin. Note that the failures took place near the end plugs.



Capsule Inner
Surface Near Top
of Fuel Pin



Capsule Outer
Surface Near Top
of Fuel Pin

Figure 10. Photographs of capsule inner and outer surfaces near the top of the fuel pin. There are no indications of any large surface build-ups; only a mild discoloration.

Figure 11 is a graph showing the capsule outer diameter and fuel pin outer diameter (less end plugs) showing that the greatest deviations from the nominal assembly dimensions were near the end plugs. Figure 12 is a graph of the capsule inner diameter and the fuel pin outer diameter illustrating the axial radial gap. The bottom end plug was measured at one location and the top end plug was measured at 2 locations. These measurements imply that the SiC cladding and the end plugs swelled beyond the design calculations and exerted considerable force on the capsule wall. The measurements were difficult to make because of the poor surface quality of the components; also, some relaxation (dimensional increase) of the components may have happened during disassembly, thus the apparent negative gap in some regions. Further work, beyond this PIE report, will have to be done to determine the material's behavior, the actual operating temperature, and the mechanical stresses.

2.8 Segment the Fuel Pin for MET/SEM and Radiochemical Samples

Because of the poor condition of the fuel pin and the fuel sliding out, the fuel pin samples were changed:

1. A ring sample was cut from the cladding about 1" from the bottom plug (estimated) and used to make a MET mount.
2. A sample was taken from the approximate middle of the top end plug and used to make a MET mount.
3. A random sample of the fuel stack was taken and analyzed for burn-up.

The ring MET mount is shown in Figure 13. Difficulties were encountered in polishing this mount and it is shown for qualitative purposes only. The structure of the cladding is apparent, the inner SiC layer, the fiber center, and the SiC outer layer. Resources were not sufficient for a second try.

The full view top end plug MET mount is shown in Figure 14. Only half of the plug could be brought into view during the grinding and polishing; it either shifted slightly during mounting or a portion of it chipped off during cutting and grinding. The full cladding cross section is apparent; much of it is in poor condition and the fibers are not evenly distributed; see Figure 15. It is difficult to tell if the apparent porosity is actually present or due to chip out during preparation as this material was friable. Using image analysis software and the source photo for Figure 14, the diameter of the plug segment was estimated to be 0.312"; the nominal dimension is 0.322" at the ½ length position. The plug is tapered and ranges from 0.310 to 0.333" in diameter. This suggests that the cut was actually nearer the bottom of the plug or the plug shrank. The outer diameter of the clad at the cut point was 0.397", the nominal value is 0.393"; this number agrees well with Figure 12. The inner diameter of the clad was 0.336"; the nominal value is 0.329". The inner diameter of the composite layer was estimated at 0.364" and the outer region at 0.380". The plug sealing material is not apparent in this photo, but it may have pulled out during the grinding and polishing, thus we have no information on its detailed behavior.

The local cladding layer regions are also of interest as they can be used to get better estimates of the layer thicknesses; see Figure 16 which shows the three regions: outer SiC seal layer, composite layer, and inner SiC seal layer. The nominal dimensions are: outer SiC seal layer 0.004" thick, the composite layer 0.014" thick, and the inner seal layer 0.014" thick. Estimates of these layer thicknesses from the MET mount, using the same image analysis software as above, are outer SiC seal layer 0.0087" thick, composite layer 0.0084" thick, and inner seal layer 0.014".

Together, these values indicate that the clad expanded outward consistent with the previous measurement, but the measured values for the layer thickness are quite different than the nominal values for the composite region and the outer SiC seal layer. Given this data and the fiber inconsistencies in Figure 15, the construction of the cladding may have been different than the nominal design. If the porosity in the composite layer is real and greater than pre-irradiation, then the expansion of the composite region may have driven the outward expansion, stressing the seal layers and cracking/breaking them. Neither mount showed signs of fuel clad interaction.

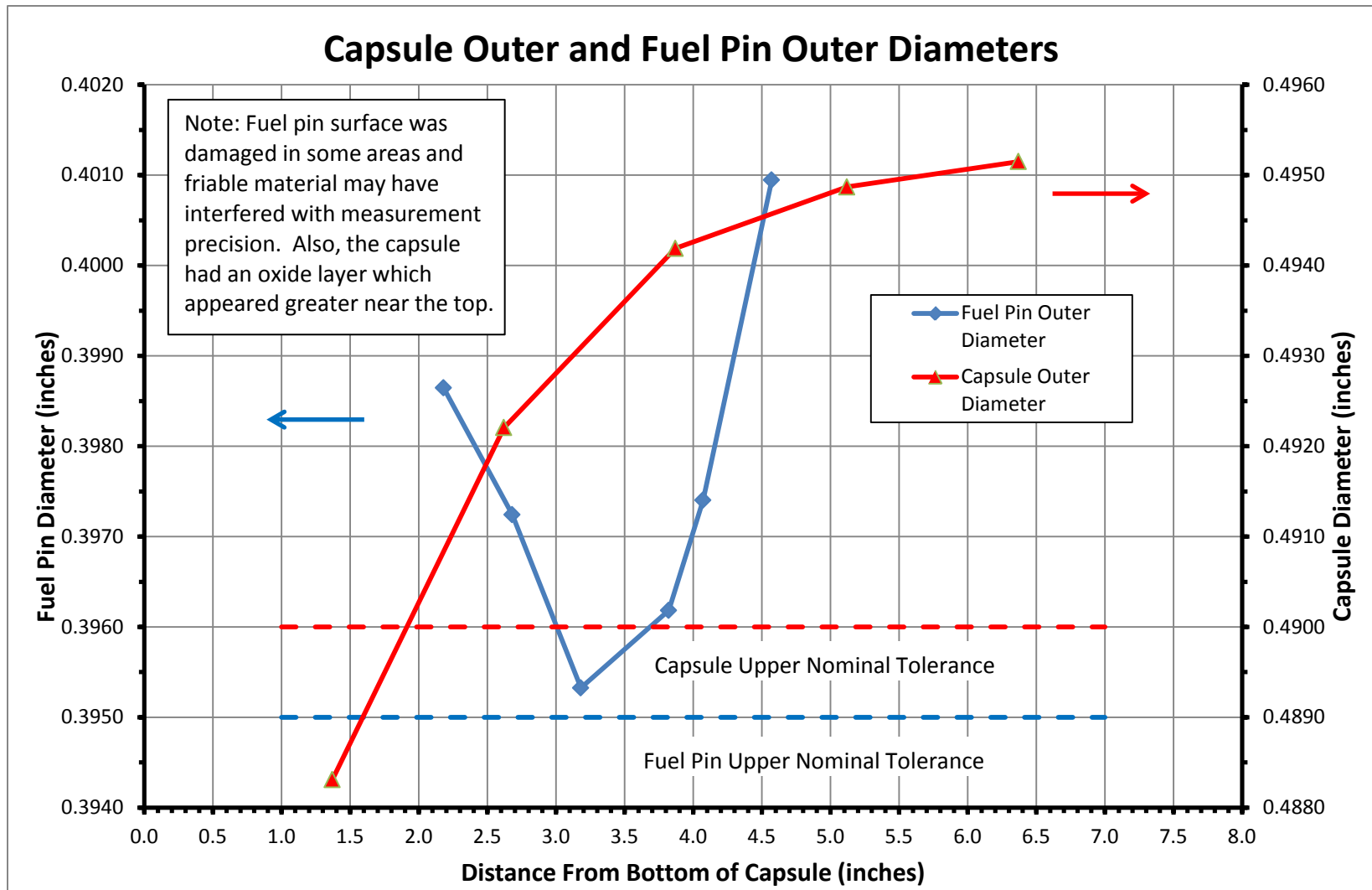


Figure 11. Outer capsule and fuel pin diameters. Note the increases near the fuel pin ends. This graph does not include the fuel pin broken off end plugs.

Capsule Inner and Fuel Pin Outer Diameters

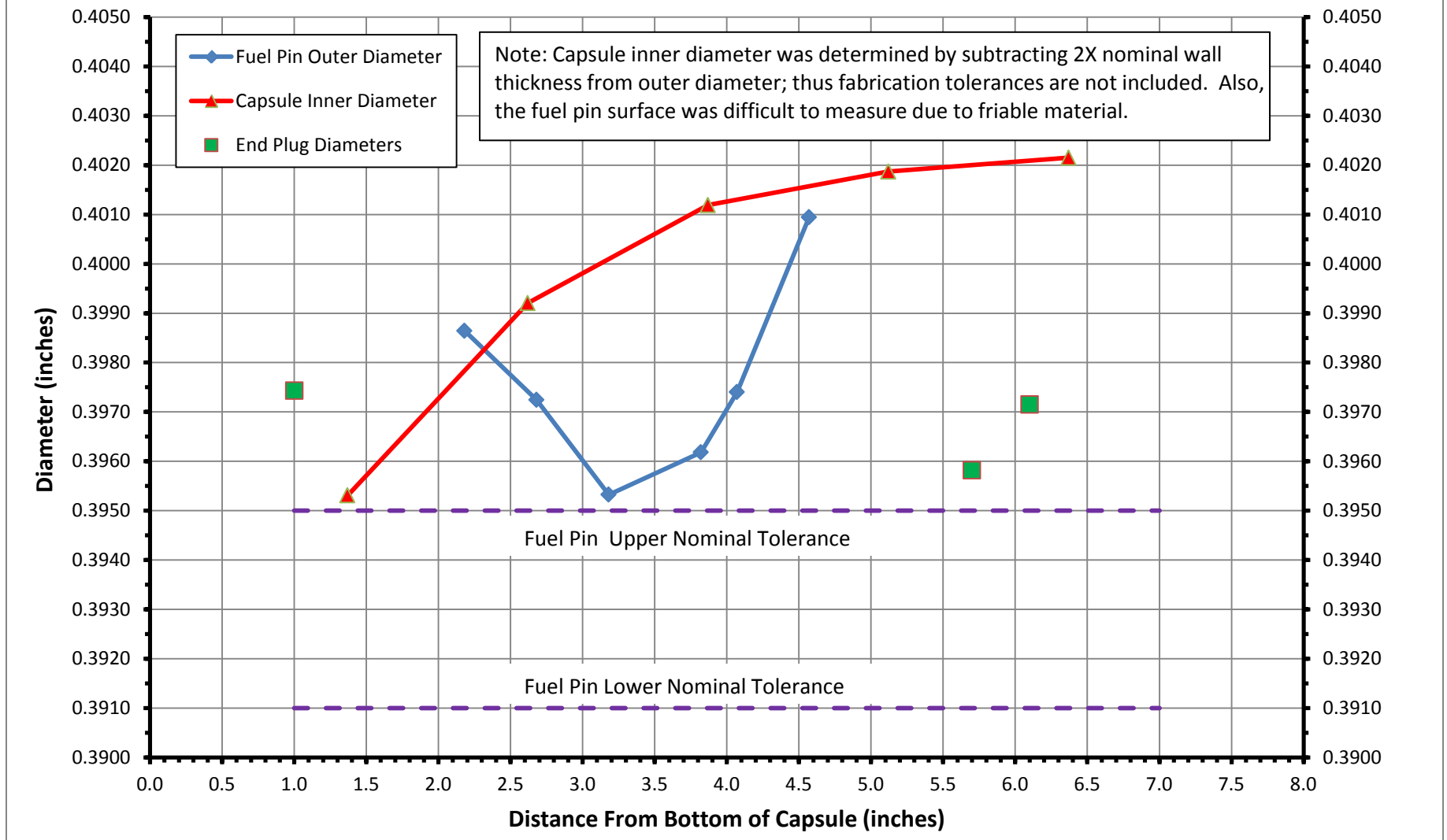


Figure 12. Capsule inner and fuel pin outer diameters illustrating gap.



Figure 13. Clad ring sample about 1" from bottom. Difficulties were encountered in the preparation of this mount; however, some detail about the structure of the clad can be gleaned. Because of the poor nature of this mount, no information about the cracking is certain since the cracks may have occurred during the preparation; however, the clad was in poor condition prior to mounting so it is likely that some physical damage occurred during irradiation.



Figure 14. Cross section of top end plug and adjacent cladding. Note the poor condition of the cladding and the uneven distribution of the fibers at the 5 o'clock position. The end plug either shifted or chipped and could not be polished flat. The cement holding the plug in is not readily apparent. The black regions are epoxy; it is difficult to tell if the SiC composite has significant porosity or if these regions are due to pull-out during preparation.

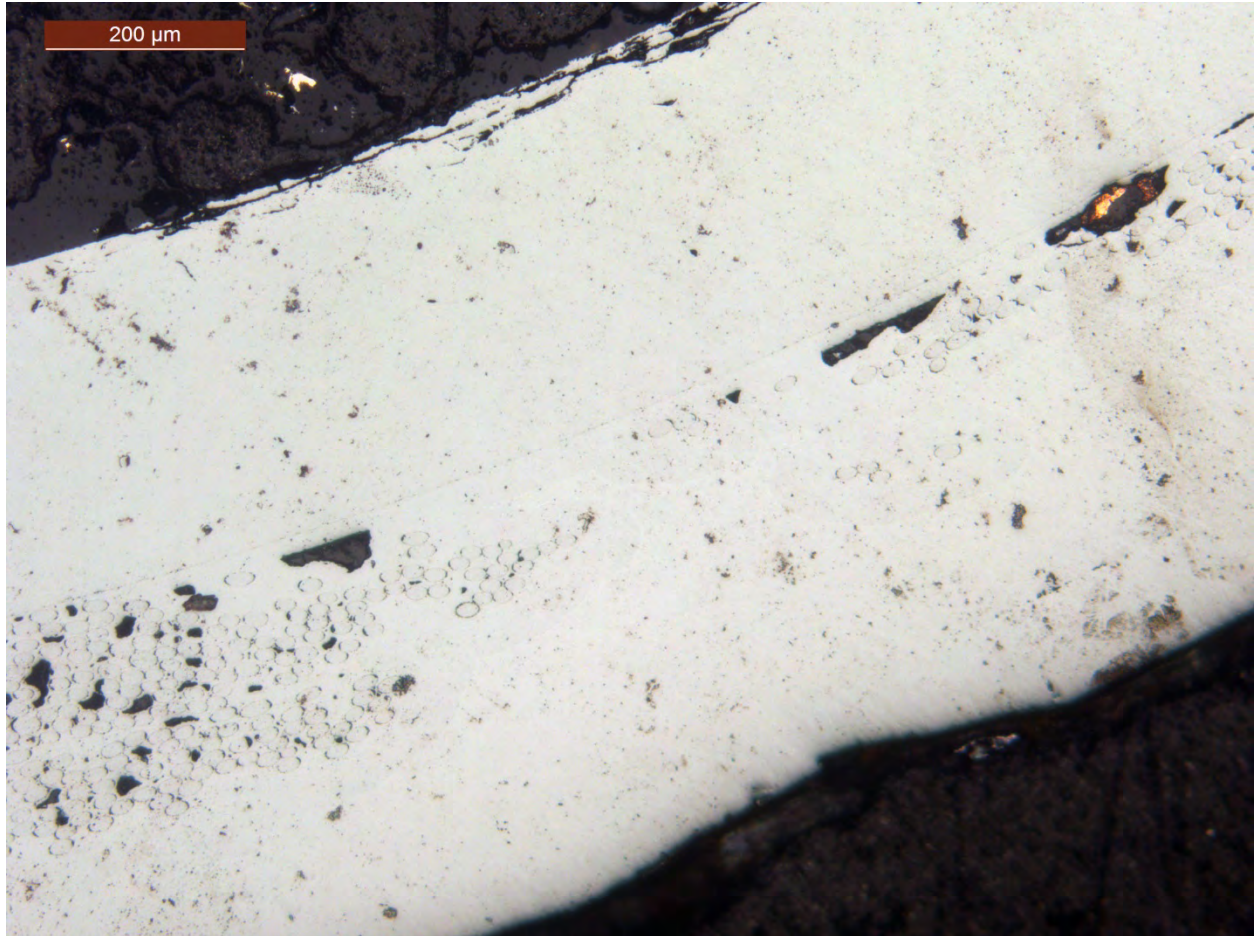


Figure 15. Close up of cladding region at 5 o'clock (Figure 14) with low fiber count.

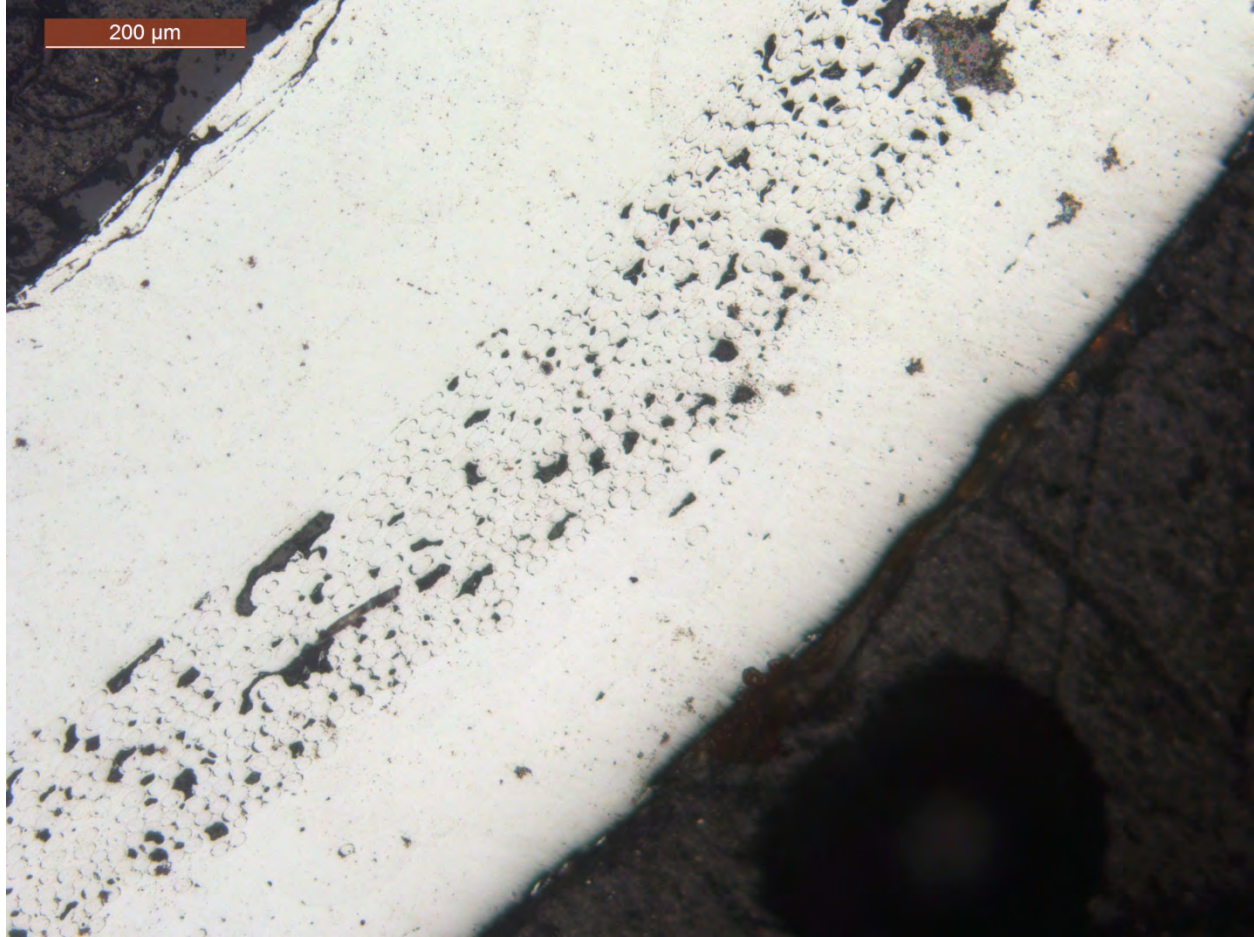


Figure 16. Cladding region at 4 o'clock (Figure 14) showing the relative thicknesses of the three cladding regions: inner SiC seal layer, composite layer, and outer SiC seal layer.

2.8.1 Measured Percent Fission (Burn-up)

The empirical determination of percent fission, uranium, plutonium, neodymium, and cesium isotopics was conducted by using Isotope Dilution Mass Spectrometry (IDMS) techniques. In addition, gamma emitting fission products were measured using high resolution gamma spectroscopy. For Nd an enriched Nd-150 standard was obtained through the DOE's National Isotope Development Center (NIDC) (which is located at ORNL). The standard's elemental assay used for the analysis was based on the measured weight of the oxide standard. The gravimetric dissolution of the standard was confirmed by reverse IDMS using an NIST Nd single element standard and high precision multi-collector ICPMS (MC-ICPMS). The Pu-242 enriched standard used was prepared from a legacy plutonium metal coupon isotopically measured by high precision MC-ICPMS and verified for elemental assay by reverse IDMS (MC-ICPMS) using IRMM-082 with a plutonium-239 spiked nitrate solution. The enriched uranium standard used was CRM 111A purchased from New Brunswick Laboratory (NBL). For cesium, a NIST traceable natural Cs-133 obtained from a commercial vendor was used. The gamma systems were calibrated using a NIST traceable multi-nuclide standard obtained from a commercial vendor.

The determined isotopics in weight percent and assays for each of the elements are listed in Table 4. Detailed evaluations of the combined standard uncertainties (CSU) for these results were performed with the use of GUM Workbench software, version 2.4 (Metrodata, GmbH). GUM Workbench incorporates the principles set forth in the ISO/IEC document *Guide to the Expression of Uncertainty in Measurement* and provides a systematic way to capture the uncertainties associated with each step of an analytical methodology such as IDMS. In general, from these evaluations it was determined that the IDMS assay for all elements have a relative 2-sigma CSU of $\pm 2\%$. The relative CSU for the isotopic concentrations, which is dependent on the count rate measured at the ICPMS, generally are $\pm 2\%$ for the major isotopes and ± 3 to 5% for the minor isotopes. The calculated 2-sigma uncertainties (absolute) are shown for each of the values reported.

For gamma spectrometry measurements sample aliquots were diluted using nitric acid to obtain a count rate with $<10\%$ deadtime. A Canberra Genie-2000 Data Acquisition System in conjunction with High Purity Germanium Detectors and Canberra Lynx modules was used for the measurement and data reductions. Results are reported in Table 5 below with dates and times measured and the calculated 2-sigma standard counting errors.

The burnup was calculated using the guidance established in [7] ASTM E 321-96, *Standard Test Method for Atom Percent Fission in Uranium and Plutonium Fuel (Neodymium-148 Method)*. The overall effective fractional fission yield for Nd-148 was determined to be 0.01706 using the weighted average of percent thermal fissions from U-235, Pu-239, Pu-241, and fast fission from U-238 per the guidance in the standard method. Table 6 lists the experimentally measured percent fission (%). The result is expressed in units of percent fission (%) and GWd / MT.

Evaluation of the CSU for the Nd-148 based fission result was performed with the use of GUM Workbench software. From this evaluation it was determined that the Nd-148 burn-up values have a relative 2-sigma CSU of $\pm 2\%$.

Table 4. Results: Assay (g / g Fuel) and Isotopics (wt. %) by IDMS

Project ID	SiC B4 Fuel	
	Result	Uncertainty
<i>Date Measured</i>	4/2/2014	
Cs (elemental)	1.503E-03	0.003E-03
Cs-133	47.1555%	0.2782%
Cs-134	0.5962%	0.1908%
Cs-135	9.7315%	0.0156%
Cs-137	42.5168%	0.3231%
<i>Date Measured</i>	03/07/2014	
Nd (elemental)	2.479E-03	0.003E-03
Nd-142	0.4523%	0.0077%
Nd-143	25.3541%	0.2789%
Nd-144	27.9079%	0.2149%
Nd-145	19.2076%	0.2113%
Nd-146	15.9333%	0.1753%
Nd-148	8.6213%	0.1121%
Nd-150	2.5235%	0.0252%
<i>Date Measured</i>	03/04/2014	
U (elemental)	8.634E-01	0.013E-01
U-234	0.0040%	0.0014%
U-235	2.7124%	0.0461%
U-236	0.3746%	0.0045%
U-238	96.8729%	0.4844%
<i>Date Measured</i>	03/05/2014	
Pu (elemental)	3.073E-03	0.006E-03
Pu-238	0.1829%	0.0027%
Pu-239	77.7460%	0.2332%
Pu-240	19.3776%	0.1124%
Pu-241	2.3807%	0.0231%
Pu-242	0.3128%	0.0018%

Table 5. Results: Radionuclide Bq count rates and their equivalent mass fractions (g/g Fuel)

Radionuclide	Measured Bq rate (Bq/g) [02/26/2014]	Uncertainty (2σ)	Conversion 1g = x Bq	Equivalent meas. mass (g/gFuel)
Nb-95	9.90E+08	3.0%	1.45E+15	6.81E-07
Zr-95	6.40E+08	3.1%	7.95E+14	8.05E-07
Ru-103	2.80E+07	14.3%	1.20E+15	2.34E-08
Ru-106	1.70E+09	5.9%	1.23E+14	1.39E-05
Sb-125	5.60E+07	7.1%	3.84E+13	1.46E-06
Cs-134	4.20E+08	1.4%	4.78E+13	8.78E-06
Cs-137	1.90E+09	5.3%	3.21E+12	5.92E-04
Ce-141	1.10E+07	18.2%	1.06E+15	1.04E-08
Ce-144	1.10E+10	9.1%	1.18E+14	9.34E-05
Eu-154	2.20E+07	9.1%	9.99E+12	2.20E-06

Table 6. Measured Percent Fission (Burn-up)

Project ID	(%)	(GWd / MTHM)
SiC B4 Fuel	2.28	21.91

2.8.2 Summary of Simulation Calculations and Burn-up Determinations

The comparison of calculated and measured mass fractions for selected important isotopes of Nd, U, and Pu is tabulated in Table 7. The dates on which the IDMS measurements were completed are indicated in Table 4 for each element. The calculated mass fractions are for the simulated average composition of the totality of all 10 fuel pellets in the B4 fuel pin.

Table 7. Comparison of Selected Calculated and Measured (IDMS) Nuclide Mass Fractions

Element/Nuclide	Mass fraction (calc) (g/gFuel)	Mass fraction (measured) (g/gFuel)	C/M
<i>Nd (elemental)</i>	<i>2.034E-03</i>	<i>2.479E-03 ±0.12%</i>	<i>0.821</i>
Nd-142	5.289E-07	1.121E-05 ±1.8%	0.047
Nd-143	5.261E-04	6.285E-04 ±1.2%	0.837
Nd-144	5.345E-04	6.918E-04 ±0.89%	0.773
Nd-145	3.901E-04	4.762E-04 ±1.2	0.819
Nd-146	3.222E-04	3.950E-04 ±1.2%	0.816
Nd-148	1.827E-04	2.137E-04 ±1.4%	0.855
Nd-150	7.832E-05	6.256E-05 ±1.1%	1.252
<i>Cs(elemental)</i>	<i>1.362E-03</i>	<i>1.503E-03 ±0.2%</i>	<i>0.906</i>
<i>Cs-133</i>	<i>6.2334E-04</i>	<i>7.087E-04 ±0.79%</i>	<i>0.880</i>
<i>Cs-134</i>	<i>9.6899E-06</i>	<i>8.9609E-06 ±32.2%</i>	<i>1.081</i>
<i>Cs-135</i>	<i>1.5546E-04</i>	<i>1.4626E-04 ±0.36%</i>	<i>1.063</i>
<i>Cs-137</i>	<i>5.7356E-04</i>	<i>6.390E-04 ±0.96%</i>	<i>0.898</i>
<i>U(elemental)</i>	<i>8.623E-01</i>	<i>8.724E-01 ±0.15%</i>	<i>0.988</i>
U-234	3.449E-04	3.490E-05 ±35.2%	0.988
U-235	2.554E-02	2.366E-02 ±1.85%	1.079
U-236	3.027E-03	3.268E-03 ±1.35%	0.926
U-238	8.334E-01	8.451E-01 ±0.65%	0.986
<i>Pu(elemental)</i>	<i>2.646E-03</i>	<i>3.073E-03 ±0.19%</i>	<i>0.861</i>
Pu-239	2.186E-03	2.389E-03 ±0.495%	0.915

Based on the average ¹⁴⁸Nd build-up mass fraction calculation for the B4 fuel pin, the average calculated burn-up from the hybrid reactor physics and isotopics model is 18.8 GWd/MTHM (slightly higher than the initial prediction). Further assessments of the burn-up based on calculated Nd isotope mass fractions (using methods documents in Ref. 8) lead to a fuel pellet burn-up level of 19.5 GWd/MTHM (within the tolerance of the first prediction).

In addition to the comparisons between average and measured IDMS results for Nd, U, and Pu isotope mass fractions, a comparison is made between measured mass fractions (converted from measured Bq count rates) as seen in Table 8. The calculated mass fractions tabulated in Table 7 and Table 8 were determined for the exact same date as the IDMS or counting rate measurements, to account for any decay,

depletion, or generation of the nuclides. (As indicated in Table 5, the radionuclide counting rate measurements were performed on 02/26/2014.)

The C/M ratios in Table 8 for the more important radionuclides show good agreement. The measurements for Cs-137 from IDMS and from the count rate measurements are somewhat different; this results in a Cs-137 C/M ratio of 0.90 based on the IDMS measurement and a C/M ratio of 0.97 based on the Bq count rate measurements for Cs-137.

Table 8. Comparison of Calculated and Measured Radionuclide Mass Fractions

Radionuclide	Mass fraction (Calculated) (g/g Fuel)	Mass fraction (Measured) (g/g Fuel)	C/M
Nb-95	9.80E-07	6.81E-07 ±3.0%	1.44
Zr-95	8.15E-07	8.05E-07 ±3.1%	1.01
Ru-103	2.36E-08	2.34E-08 ±14.3%	1.01
Ru-106	1.53E-05	1.39E-05 ±5.9%	1.10
Sb-125	1.78E-07	1.46E-06 ±7.1%	0.12
Cs-134	9.48E-06	8.78E-06 ±1.4%	1.08
Cs-137	5.74E-04	5.92E-04 ±5.3%	0.97
Ce-141	1.03E-08	1.04E-08 ±18.2%	0.99
Ce-144	9.57E-05	9.34E-05 ±9.1%	1.02
Eu-154	2.97E-06	2.20E-06 ±9.1%	1.35

Radiochemical count rate and IDMS measurement results (previous section) show a burn-up level of 21.91 GWd/MTHM based on the Nd-148 concentration measurement. The calculationally-predicted average burn-up level for the fuel material in fuel pin B4 is 18.8 GWd/MTHM based on the calculated average Nd-148 concentration. There is some variation in the burnup of the 10 pellets that comprise the B4 fuel pin. Illustrative of this, the calculated burnup for one of the fuel pellets based on its (calculated) Nd-148 concentration is somewhat higher at 19.5 GWd/MTHM.

It is a known phenomenon in the irradiation of LEU UO₂ fuel pellets that rim effects [9, 10] result in sharp increases in burn-up levels, and Pu and Nd isotope mass fractions, in the outer annular zones of the fuel pellets. These rim effects are usually quite prominent at high fuel burnup levels, but are non-negligible at moderate burnup levels in the 20 GWd/MTHM range as seen in Figure 17 and Figure 18.

As mentioned earlier in this report, the B4 fuel readily fell out of the SiC cladding tube in a crumbled form. It was not actively homogenized (crushed and mixed) so there is the possibility of a range of apparent measured burn-up levels depending on the samples that were chosen. Of the actual approximately 55.353 g of fuel mass from the 10 irradiated fuel pellets from fuel pin B4, about 5.4 g (equivalent to about a single pellet's mass) was selected for radiochemical analyses.

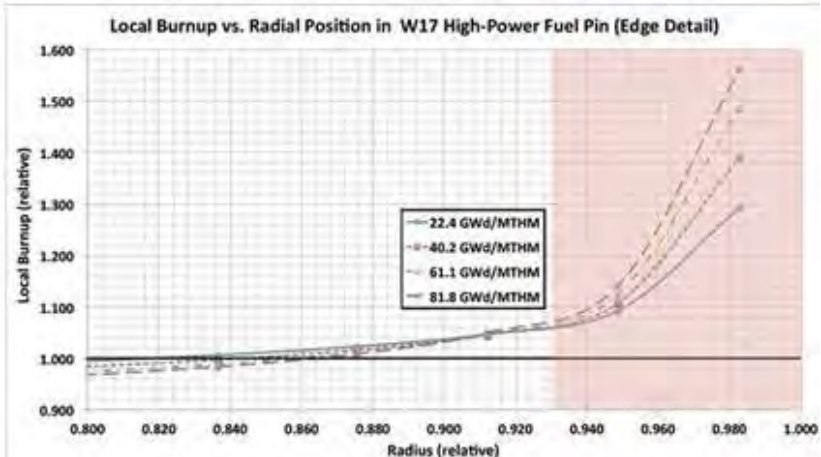
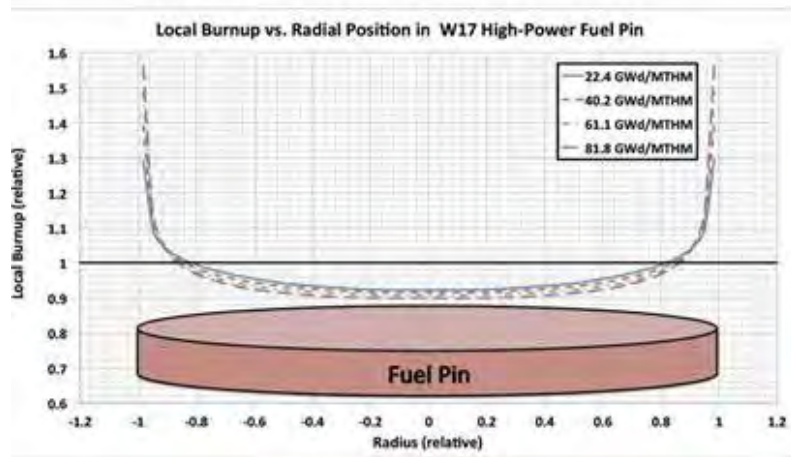


Figure 17. From Ref. 9, the rim effect in the radial fuel burn-up profile of an irradiated fuel pellet, for average pellet burn-ups from 20 to 80 GWd/MTHM. The effect is not insignificant, even for burn-up of 20 GWd/MTHM .

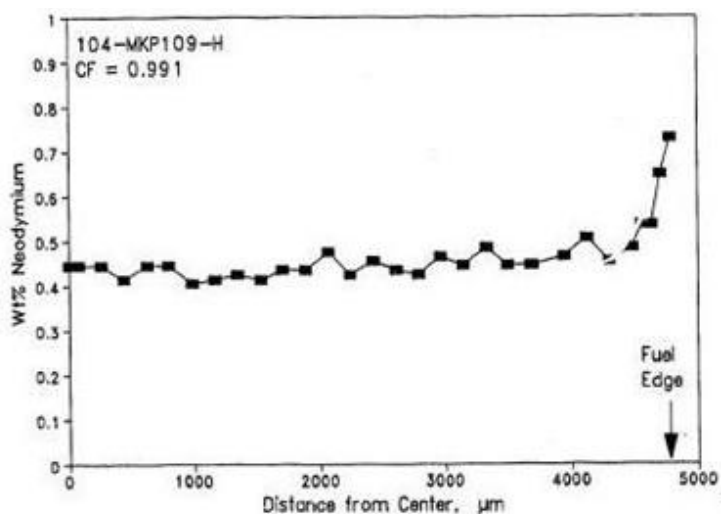
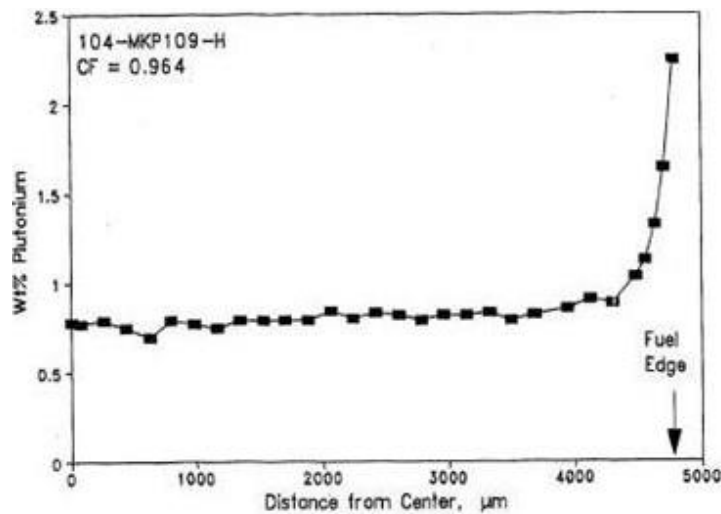


Figure 18. Plutonium and Neodymium Concentrations across the radius of a fuel pellet in the Ref. 10 measurements: Illustration of the rim effect in irradiated pellets.

3. PIE CONCLUSIONS

The SiC clad swelled during irradiation and placed pressured on the outer stainless steel capsule as indicated by dimensional measurements; the extent of the swelling was such that the fuel pin could not be easily removed and had to be cut out. Prior to capsule opening and fuel pin retrieval, a gamma scan revealed that all the capsule and pin components were in their expected locations. Sometime during the irradiation the pin seal failed and leaked fission gas to the capsule plenum; thus, an accurate measurement of fuel fission gas release could not be obtained.

After opening, the fuel pin was found to be broken into 3 pieces. It is not clear whether the pin was broken during irradiation or failed during opening. It was clearly in a poor state. The fuel was loose in the clad and all of it slid out during handling; thus a MET mount with both fuel and cladding could not be obtained. No macro signs of fuel/cladding interactions were noted, but the clad swelling eliminated any hard fuel/clad contact. MET mounts showed that the clad expanded outward and that the actual construction may have been somewhat different than the nominal design.

The comparisons of nuclide mass fractions for Nd, U, and Pu from IDMS determinations and of radionuclides from count rate measurements to the calculated mass fractions from the reactor physics/depletion model was seen generally to be good. In addition, the comparison of calculated to measured molar fraction ratios for Xe and Kr from the punctured fuel pin B4 steel containment can was very good.

Radiochemical measurement results (previous sections) show a burn-up level of 21.9 GWd/MTHM based on standard Nd-148 concentration assessments. The calculated average fuel pin burnup level for B4, based on the hybrid MCNP5.150/SCALE 6.1 methodology simulation calculations, was predicted to be 18.8 GWd/MTHM on the basis of the calculated pin-averaged Nd-148 concentration.

4. ACKNOWLEDGEMENTS

The authors wish to acknowledge the useful help Jeremy Busby and Gary Bell for management support, from the Building 3525 staff, (especially R.M. Smith) for their help with this PIE work, from T.A. Dyer and C. Porter for their help with the MET preparation work, from Jeff Delashmitt and Rob Smith for the hot cell dissolutions, from Tammy Keever and Ben Roach for the burn up isotopic measurements, and the radiochemical staff at Buildings 4501 and 7920 for their help in handling the radiochemical samples and conducting the isotope and gas analysis.

5. REFERENCES

1. L.J. Ott, G.L. Bell, R.J. Ellis, J.L. McDuffee, R.N. Morris, *Irradiation Of SiC-Clad Fuel Rods In The HFIR*, Oak Ridge National Laboratory, paper published in the Proceedings of Top fuel 2013, Charlotte, NC, September 15-19, 2013.
2. D.J. Spellman, G.L. Bell, R.N. Morris, R.J. Ellis, D.S. Hamm, and L.J. Ott, *FY12 HFIR Irradiation and Testing of Fueled Silicon Carbide Cladding*, ORNL/LTR-2012/470, Oak Ridge National Laboratory, Oak Ridge, Tennessee, September 2012.
3. R.J. Ellis, *Neutronics and Heat Generation Calculations in Support of the Thermal Neutron Fuel Irradiation Facility*, C-HFIR-2009-011, Oak Ridge National Laboratory, November 2009.
4. R.J. Ellis, J.C. Gehin, J.L. McDuffee, R.W. Hobbs, *Analysis of a fast spectrum irradiation facility in the high flux isotope reactor*, Paper 533, in *Proc. of PHYSOR'08 American*

- Nuclear Society International Conference on the Physics of Reactors “Nuclear Power: A Sustainable Resource,”* September 14–19, 2008, Interlaken, Switzerland.
5. D.J. Spellman, J.L. McDuffee, R.J. Ellis, D.J. Heatherly, R.W. Hobbs, L.J. Ott, K. Thoms, ***Final Design Description of a Light Water Fuel Test Irradiation Facility in the High Flux Isotope Reactor***, Oak Ridge National Laboratory, Project Report, August 2012.
 6. L.J. Ott, B.B. Bevard, R.J. Ellis, J.L. McDuffee, and D.J. Spellman, ***Advanced Fuel/Cladding Testing Capabilities in the ORNL High Flux Isotope Reactor***, Proceedings of TopFuel 2009, Paris, France, 6–10 September 2009.
 7. ASTM E 321-96, ***Standard Test Method for Atom Percent Fission in Uranium and Plutonium Fuel (Neodymium-148 Method)***, ASTM International, West Conshohocken, PA, USA.
 8. J.S. Kim, Y.S. Jeon, S.D. Park, B.C. Song, S.H. Han, J.G. Kim, Korea Atomic Energy Research Institution paper, ***Dissolution and Burnup of Irradiated U-Zr Alloy Nuclear Fuel by Chemical Methods***, Nuclear Engineering and Technology, Vol. 38, No.3, April 2006.
 9. B.J. Ade, H.J. Smith, I.C. Gauld, ***Generation of Source Terms for High Burnup PWR and BWR Fuel in Long Term Cask Storage***, Oak Ridge National Laboratory letter report to USNRC, ORNL/LTR-2012/217, November 29, 2012.
 10. R.J. Guenther, D.E. Blahnik, U.P. Jenquin, J.E. Mendel, L.E. Thomas, C.K. Thornhill, ***Characterization of Spent Fuel Approved Testing Material – ATM-104***, Pacific Northwest Laboratory report, PNL-5109-104, December 1991.